NASA MEMO 1-10-59L

NASA

MEMORANDUM

A HYDROGEN PEROXIDE HOT-JET SIMULATOR

FOR WIND-TUNNEL TESTS OF

TURBOJET-EXIT MODELS

By Jack F. Runckel and John M. Swihart

Langley Research Center
Langley Field, Va.

NATIONAL AERONAUTICS AND SPACE ADMINISTRATION

WASHINGTON

February 1959

NATIONAL AERONAUTICS AND SPACE ADMINISTRATION

MEMORANDUM 1-10-59L

A HYDROGEN PEROXIDE HOT-JET SIMULATOR FOR WIND-TUNNEL TESTS OF TURBOJET-EXIT MODELS

By Jack F. Runckel and John M. Swihart

SUMMARY

A turbojet-engine-exhaust simulator which utilizes a hydrogen peroxide gas generator has been developed for powered-model testing in wind tunnels with air exchange. Catalytic decomposition of concentrated hydrogen peroxide provides a convenient and easily controlled method of providing a hot jet with characteristics that correspond closely to the jet of a gas turbine engine.

The problems associated with simulation of jet exhausts in a transonic wind tunnel which led to the selection of a liquid monopropellant are discussed. The operation of the jet simulator consisting of a thrust balance, gas generator, exit nozzle, and auxiliary control system is described. Static-test data obtained with convergent nozzles are presented and shown to be in good agreement with ideal calculated values.

INTRODUCTION

It has long been recognized that jet effects are responsible for a number of the differences between drag, stability, and loads results obtained in flight tests and in the usual wind-tunnel investigations. Because of the importance of these effects, methods for simulating jets were developed for subsonic tunnels (ref. 1), for supersonic tunnels (refs. 2 and 3), and for rocket models (ref. 4). The problem of simulation at transonic speeds, however, was found to be more difficult because of the much greater importance of support interference effects (refs. 5 and 6). The use of air or air-fuel-combustion systems (ref. 7) would require large induction pipes which must be enclosed in thick support members and would lead to increased transonic support interference.

A simulation scheme that would permit detailed study of installation problems and jet interference effects for complete or essentially complete models was desired. The primary characteristics desired were large model

size, minimum support interference, and sufficiently close duplication of turbojet exhaust characteristics to permit valid studies of the interactions of such a jet with both internal and external flows.

After consideration was given to several methods of producing a hot jet that would simulate the characteristics of turbojet-engine exhausts, as well as to a system that would require a minimum of space inside the model and support, the liquid monopropellant hydrogen peroxide was selected. The literature revealed that hydrogen peroxide had been used as a successful gas generator for turbopump turbine drives (ref. 8). Extensive information concerning experience with the liquid as a propellant was available (ref. 9), so that little development work appeared to be required to adapt this system for research.

The purpose of this paper is to describe the development of a hydrogen peroxide turbojet-engine simulator, which can be used for powered model testing in wind tunnels with air exchange, in supersonic blowdown tunnels, or in free flight, and to indicate the necessary associated equipment for use in the wind tunnel. The results of static tests on some turbojet-exit-tailpipe configurations obtained by using the hydrogen peroxide simulator are discussed.

SYMBOLS

A jet exit area, sq ft

C_F thrust coefficient, $F_j/q_\infty A$

$C_{F,o}$ static thrust coefficient, $F_j/p_o A$

C_d mass-flow discharge coefficient, w/w_i

d diameter

F_j measured jet thrust

F_i ideal thrust for complete isentropic expansion of primary flow,

$$w\sqrt{\frac{2R}{g}\frac{\gamma}{\gamma-1}T_{t,j}\left[1-\left(\frac{p_o}{p_{t,j}}\right)^{\frac{\gamma-1}{\gamma}}\right]}$$

$F_{i,c}$ ideal convergent nozzle thrust, $\frac{w}{g}\sqrt{\gamma g R \frac{2}{\gamma + 1} T_{t,j}} + A(p_j - p_o)$

g acceleration due to gravity, ft/sec^2

M Mach number

p static pressure, lb/sq ft

p_t total pressure, lb/sq ft

q dynamic pressure, lb/sq ft

R gas constant, ft/^oR

r average radius of curvature of jet boundary

T temperature, ^oR

t static temperature, ^oF

t_t total temperature, ^oF

V velocity, ft/sec

w measured weight flow, lb/sec

w_i ideal weight flow for choked exit, $p_{t,j} A \left(\frac{2}{\gamma + 1}\right)^{\frac{\gamma+1}{2(\gamma-1)}} \sqrt{\frac{\gamma g}{R T_{t,j}}}$

x distance from decomposition-chamber inlet

γ ratio of specific heat at constant pressure to specific heat at constant volume

δ angle between jet axis and tangent to free jet boundary at nozzle lip, deg

ρ mass density, slugs/cu ft

Subscripts:

c convergent nozzle

j jet

o	barometric
t	total
∞	free stream

FLOW-SIMILARITY CONSIDERATIONS

A propulsive jet affects the airplane through both direct reactions and interferences. In certain free-flight and wind-tunnel stability and performance investigations (refs. 4 and 10), complete simulation of both items may be required. For most wind-tunnel investigations, however, it is only necessary to reproduce the interference effects. Primary attention was focused on this more restricted problem in the development of the jet simulation system considered herein. Simulation of the jet intake flow may not be necessary if the external flow field in the vicinity of the exit is similar to that of the airplane. Numerous drag investigations have provided a broad background of information concerning the interference effects of intake flow in the transonic-speed range.

A convenient approach in an analysis of interference effects due to a propulsive jet is to break down the jet flow into two regions: the region of the jet bulb immediately downstream of the exit and the trailing mixing region. With a given set of external flow conditions the initial shape of the jet boundary is determined mainly by the ratio of specific heats γ and nozzle exit pressure ratio p_j/p_∞ of the jet flow (ref. 11). Results from numerous investigations at the Langley Laboratory have indicated that duplication of the slope of this segment of the jet boundary is all that is required in studies of the base and boattail drag of afterbodies without appreciable flow separation and external interference effects associated with the initial (exit) shock. This finding is of great practical significance with regard to simulator selection, inasmuch as it permits the use of a jet with an incorrect ratio of specific heats for a limited range of investigations, because the correct initial boundary shape still can be obtained by operating the simulator at some arbitrary exit pressure ratio.

The characteristics of the jet downstream of the initial expansion are determined by a number of internal jet-flow properties in addition to the specific-heat ratio and the nozzle exit pressure ratio. For example, when the external stream is supersonic, the internal jet shock penetrates the mixing boundary into the free stream and forms a second external shock system downstream of the exit shock (ref. 12). When the external flow is subsonic, the internal shock, instead of penetrating into the external flow, reflects from the interface, so that the familiar "shock diamonds" are formed and a somewhat wavy jet boundary results (ref. 11). In either case, simulation of the downstream shock structure

obviously involves reproducing the exit Mach number and nozzle geometry, as well as exact representation of the exit pressure ratio and ratio of specific heats. This degree of simulation appears to be adequate for most studies of downstream shock interference effects.

Complete representation of the interference effects of the downstream jet requires simulation of the mixing processes along the jet boundary, in addition to all the items mentioned previously. These mixing processes are governed by the viscosities, momentums, and heat-transfer rates of the local elements of mixing flow so that complete simulation involves essential representation of the actual jet engine exhaust. This degree of simulation obviously is not needed in most flow-field studies. It may be justified, however, in investigations wherein flow entrainment along the jet boundary and jet-area-displacement effects are important factors. For example, changes in jet temperature have been found to have significant effects in investigations of afterbodies with appreciable flow separation and investigations of afterburner arrangements. In such cases, departures from complete simulation can only be justified on the basis of experience.

Preliminary studies on jet effects at the Langley and Lewis Laboratories of the NACA considerably clarified the nature of the downstream-mixing and jet-interference effects due to changes in exhaust gas properties. After study of these findings and the flow-similarity considerations previously discussed, it was decided that the jet-simulation system to be used in the Langley 16-foot transonic tunnel must provide a hot jet which would closely represent the flow conditions in the immediate vicinity of the nozzle exit and would reasonably simulate the downstream flow-field effects, yet would not compromise the necessary minimization of the support-interference effects.

SUITABILITY OF HYDROGEN PEROXIDE FOR JET SIMULATION

Study of a number of possible methods of jet simulation led to selection of a monopropellant (hydrogen peroxide) rocket system as being most suitable for the use of the Langley 16-foot transonic tunnel. This system possesses the basic advantages of compactness, small supply lines, and ease of operation (the jet pressure ratio is controlled by simply varying the weight flow through the system). The products of decomposition of H_2O_2, steam and oxygen, allow safe operation in a wind tunnel. The amount of water added to the airstream would not affect the operation of either a large wind tunnel cooled by an air exchange system or a blowdown type of tunnel.

Physical Properties of Hydrogen Peroxide

Hydrogen peroxide is a clear liquid oxidizer with a high internal energy content. It is used in rocketry in concentrations between 80 and 100 percent (ref. 9). The physical properties of H_2O_2 are listed in references 9 and 13. Some of the physical properties of the mixture of H_2O_2 decomposition products are shown in figure 1. The liquid can be decomposed catalytically by many heavy metals and their salts. The chemical mechanism of hydrogen peroxide decomposition by silver catalyst is discussed in reference 14. Some incomplete decomposition has been experienced with concentrations of hydrogen peroxide lower than 90 percent when a silver catalyst bed was used; therefore, only this commercially available concentration was considered. All further reference in this paper to H_2O_2 is for a concentration of 90 percent hydrogen peroxide by weight, with the remaining weight being pure water. Decomposition of 90 percent H_2O_2 results in an increase in volume of 5,233 times with an adiabatic decomposition temperature of 1,364° F at atmospheric pressure. The molecular weight of this gas is 22.105 and the ratio of specific heats γ is 1.266. The coefficient of thermal conductivity is about 12.5×10^{-6}, and the kinematic viscosity calculated for a jet total-pressure ratio of 4.20 is about 9.2×10^{-4}.

JET-FLOW CHARACTERISTICS

In order to illustrate the suitability of a hydrogen peroxide jet for turbojet-exhaust simulation in the Langley 16-foot transonic tunnel, H_2O_2 jet flow characteristics have been calculated for three important operating conditions (take-off static thrust, high subsonic cruising, and afterburning climb flight) and are compared in table I with corresponding characteristics for an actual turbojet exhaust and for a cold air jet. The parameters held constant in the comparisons are the stream Mach number and the jet total-pressure ratio $p_{t,j}/p_\infty$. The ambient conditions chosen for the turbojet correspond to the actual flight conditions, whereas the ambient temperature and pressure chosen for the H_2O_2 simulator and cold air jet are typical values encountered in a transonic atmospheric wind tunnel. Zero intake-ducting losses, a convergent nozzle, and nozzle discharge and velocity coefficients of unity were assumed in the calculations. Jet-boundary-shape parameters were determined by use of the charts of reference 11. Jet-boundary-shape parameters for H_2O_2 were obtained by interpolation of the charts of reference 11 and are presented in figure 2.

For the operating conditions considered in table I, the initial jet-boundary-shape parameters δ and r/d_j are in reasonably close

agreement for all three types of jets in the cruising and afterburning flight conditions. The jet-bulb-radius parameter r/d_j given for the H_2O_2 simulator is lower than for the turbojet and cold air jet for the static-thrust condition. It is believed, however, that the difference shown is unimportant, because the slope of the curves of r/d_j plotted against $p_{t,j}/p_o$ tends to become infinite at jet-pressure ratios in the neighborhood of 2.5. (See fig. 2.) As in all the other cases shown, changing the operating pressure ratio by only a few tenths would result in initial jet-bulb shapes almost identical with those for the actual turbojet exhaust.

It is interesting to note that a comparison of the kinematic viscosities (a factor in the Reynolds number affecting the shear at the jet boundary) of the hydrogen peroxide jet and a turbojet exhaust shows almost perfect agreement. The coefficients of thermal conductivity which are involved in the heat transfer between the boundaries are about 10 percent higher for the hydrogen peroxide jet than for the turbojet engine. In view of the agreement of the kinematic viscosities and the coefficients of thermal conductivity of H_2O_2 and turbojet exhaust gases, interface mixing phenomena are closely simulated when the thrust coefficient (ratio of jet to stream momentums) and ratios of jet temperature to stream temperature are reasonably close. Thus, it appears that internal-external flow interactions in the trailing-wake region of interest for ejector studies can be essentially reproduced for some conditions. Inasmuch as appreciable success has been experienced in correlating ejector pumping characteristics for tests with various gases by use of a simple weight-flow parameter involving the gas temperatures and molecular weights (for example, ref. 15), the H_2O_2 jet-simulation technique would appear to be fully adequate for ejector studies over a broad range of test conditions where the thrust coefficients and temperature ratios differ appreciably from the desired turbojet exhaust values. Limits of applicability obviously will have to be established by experimental comparisons, as will the usefulness of the technique for cases in which the interference effects of the more remote jet wake are of importance.

The actual thrust provided by the jet simulator generally is of secondary importance in wind-tunnel studies. It is noted, however, that for the static, cruising, and afterburning climb conditions of table I, the pertinent thrust parameters for the H_2O_2 jet (thrust per unit jet area in the static condition and thrust coefficients for the flight conditions) are only 14.5 percent high, 5.2 percent high, and $17\frac{1}{2}$ percent low compared with the thrust parameters for the turbojet operating conditions being simulated.

APPARATUS

The apparatus required for operating a hydrogen peroxide jet simulator system must include suitable storage tanks, a flow controlling system, and a gas-generator—exit-nozzle combination.

Because of corrosive effects of H_2O_2, special materials must be used for storing and handling concentrated hydrogen peroxide. It can be stored for long periods of time in 99.6-percent pure aluminum containers which have received a special interior-surface pickling treatment to make them passive. Certain stainless steels can be used for short-time storage containers by giving them a proper passivation treatment. Reference 16 describes the passivation treatments that can be used on suitable materials. Since hydrogen peroxide is not compatible with many organic and inorganic materials, extreme caution must be used to prevent contact with these materials. Explosive mixtures can be formed with hydrocarbons such as gasoline and alcohol. Reference 16 contains safety precautions for handling and storing hydrogen peroxide. The use of concentrated H_2O_2 as a propellant requires special equipment and acceptable types are described in references 16 and 17.

Storage and Supply System

The hydrogen peroxide storage-tank farm at the Langley 16-foot transonic tunnel is shown in the photograph of figure 3. The tanks have a capacity of 5,000 gallons each and are constructed of 99.6-percent pure aluminum. The hydrogen peroxide storage system is equipped with temperature monitors and automatic alarm and flooding provisions in case contamination occurs and disposal of the hydrogen peroxide is necessary. The personnel, wearing special protective clothing, are shown while transferring hydrogen peroxide from a storage tank to the supply tank mounted on a trailer.

The trailer-mounted hydrogen peroxide supply system is shown in figure 4. It consists of a 1,100-gallon temporary storage tank, a hydrogen peroxide transfer pump, a 30-gallon high-pressure tank, a nitrogen pressurizing cascade, and safety water tank, pump, shower, and hoses. A sketch illustrating the operation of the trailer-mounted portable supply system is presented in figure 5. This trailer is used to transport H_2O_2 from railroad tank cars to the storage tank farm at Langley and to operate the H_2O_2 jet simulators. All transfer and supply operations can be controlled from the trailer panel or from a remote station connected with it. The hydrogen peroxide flow rate can be controlled by the amount of pressure on the system and by throttling the flow with a valve. Weight flows up to about 7 pounds per second at pressures up to 1,000 lb/sq in. are indicated on an electronic flowmeter.

Safety interlocks control the operating sequence, and desired flow rates can be established in about 10 seconds by adjusting the throttle valve while observing the flowmeter.

Jet Simulator

The present jet simulator consists of a thrust balance, gas generator, and tailpipe—exit-nozzle combination. A photograph of a hydrogen peroxide jet simulator is shown in figure 6. Details of the simulator are given in the sketch of figure 7, and some of the components are shown in figure 8. Hydrogen peroxide enters the thrust balance through a passage designed to eliminate liquid momentum and Bourdon tube effects and to minimize ambient and differential heating effects. Strain gages were mounted on webs on the sides of the vertical liquid passage. The thrust balance and decomposition chamber were machined from one block of high-temperature alloy to eliminate welds and chances of leakage.

The turbojet simulator utilizes a gas generator (fig. 7) in which the liquid enters the decomposition chamber through an inlet orifice which is designed to provide a pressure drop of about one-half the chamber pressure at the design flow rate. It has been found that this pressure drop will prevent pressure oscillations called chugging (ref. 18). The catalyst bed is made up from 20-mesh 0.014-inch-diameter wire screens of 99.6-percent pure silver activated with a samarium nitrate treatment.[1]

The hydrogen peroxide gas generator units can be made in a wide range of sizes to develop thrust outputs from 2 pounds to 400 pounds and much greater. Figure 9 shows a series of hydrogen peroxide gas generator units that have been developed for use in research models at the Langley Aeronautical Laboratory of the NACA. They range in size from the small 0.5-inch-diameter unit to the 5.25-inch-diameter unit shown at the top. These units have been developed for wing-tip reaction controls and primary jets in free-flight models, for exhaust simulators in towing-tank seaplane models, for multiengine jet-interference models, for missile-rocket-motor simulation, and for the turbojet-engine simulator described herein.

Two of the convergent exit nozzle configurations that have been statically tested with the turbojet-engine simulator are shown in figures 6 and 7. These were scaled nonafterburner nozzles corresponding to turbojet engine exits. One type of tailpipe configuration had a sonic throat (fig. 8) located directly behind the decomposition chamber, which was similar to the design used in reference 4. A perforated cone

---

[1]Catalyst bed and treatment devised by BECCO Chemical Division, Food Machinery and Chemical Corporation, Buffalo, New York.

was installed in the tailpipe of these units in order to shock the flow to subsonic speeds and create a total pressure loss. The throat was eliminated in the arrangement shown in figure 7 to reduce the internal pressure at the connection between the decomposition chamber and the tailpipe. The perforated cone was retained in some throatless configurations to damp pressure pulses of unknown origin which occurred in the tailpipe.

STATIC TESTS

The hydrogen peroxide jet-simulator system was statically tested to determine the agreement of the model-exit-nozzle characteristics with those of a turbojet engine nozzle. These tests covered a range of operation corresponding to that required for a transonic-wind-tunnel model test program.

The instrumentation used during the static tests consisted of a thrust balance, total- and static-pressure orifices located in the gas generator and in the exit-nozzle—tailpipe combination, and thermocouples located both inside the jet simulator and on the outside surface of the unit. Pressures were measured with electrical transducers and transmitted through carrier amplifiers to recording oscillographs. Thrust-balance strain-gage output was also measured on the recorder. Temperature measurements were obtained on multichannel or pen-trace self-balancing potentiometers. All tests were made by varying the flow rate of H_2O_2 through the jet-simulator system in predetermined steps of 10 to 20 seconds duration.

The estimated accuracy of the pressure measurements is ± 3 percent. Thrust measurements presented herein are estimated to be within 1 percent of full scale or about ± 4 pounds of thrust.

Internal Pressures

The first step in investigating the operation of the turbojet simulator was to determine if the design condition of a sonic exit had been met. Figure 10 shows the distribution of internal pressures along the walls of the turbojet simulator. The circular symbols are data taken with no shock-inducing devices in the tailpipe. The steady increase in static pressure at the walls and the decrease in total pressure in the passage is an indication of a series of oblique shocks in supersonic flow. The flow did not become subsonic until beyond the orifice at the 15.2-inch station, and supersonic flow persisted through the entire tailpipe for decomposition-chamber pressures slightly higher than those presented. It was decided, therefore, to install a perforated cone

(fig. 7) which was designed to induce shocks in the flow in order to produce subsonic speeds. Data from tests with this type of cone are shown in figure 10 and indicate that the perforated cone produced the desired subsonic flow. The solid line on the Mach number distribution indicates the distribution that would be obtained from the pressure measurements and the area distribution. Sonic exit conditions with the perforated cone were obtained at all pressure ratios above that required to choke the nozzle.

A multiple-tube total-pressure rake was installed in a simulator tailpipe—exit-nozzle combination at about the 16.7-inch station. The radial survey of the total-pressure distribution for several values of jet total-pressure ratio, $p_{t,j}/p_o$, is shown in figure 11. These results indicate that the total-pressure distribution is quite flat across the section, except at the highest pressure ratios. In addition, the boundary-layer thickness is relatively thin and should remain so as the flow accelerates to the exit nozzle.

Temperature Surveys

The variation of temperature, both internally and externally, along the jet simulator is shown in figure 12, at the locations indicated on the top sketch. Internal total temperatures were measured with liquid or stagnation-type thermocouples having a high temperature-recovery factor. The variation of the temperature rise through the catalyst bed is unknown, but a temperature increase of 1,320° F occurred from the void space ahead of the catalyst to the chamber measurement in back of the bed. Discoloration of the steel of the decomposition chamber indicated that most of the temperature increase occurred in the initial one-third of the bed. The temperature losses through the walls of this tailpipe were small; a decomposition temperature of 1,385° F was measured behind the catalyst bed and the stagnation temperature dropped 35° F to a value of 1,350° F at the exit measuring station. The fact that the measured decomposition temperature was higher than the theoretical value of 1,364° F for a 90 percent concentration of H_2O_2 may be the result of a higher concentration of H_2O_2, and inlet temperature and decomposition-chamber pressure higher than standard. External surface temperatures show a more gradual rise, reaching a maximum of 1,100° F at 15 inches from the inlet of the decomposition chamber. It should be pointed out that the temperature variation shown exists while H_2O_2 is being decomposed in the system. Upon shut-off, skin temperatures on the tailpipe decrease, but the temperatures at the upstream end of the decomposition chamber increase as the heat flows back into the inlet system, which has been cooled by the liquid H_2O_2 during jet operation. The temperatures of the connecting end of the thrust balance may approach 250° F, which represents a limit for strain-gage installations. It is apparent

that the residual heat of the jet simulator may be a problem when the unit is installed inside a model near instrumentation.

Flow Measurements

Static tests with atmospheric back pressure have been conducted on the jet simulator system at the Langley hydrogen peroxide jet test stand. Weight-flow measurements obtained from the liquid hydrogen peroxide flowmeter are compared in figure 13 with calculated flow rates at two jet simulator sonic nozzles of the type shown in figure 10. The total pressure and temperature measured in the decomposition chamber and in the tailpipe were used to determine the flow rates at the throat and the exit, respectively. Calculations for the exit of the 3.2-inch-diameter nozzle are not shown below a weight flow of 2.0 pounds per second, since the jet exit was not choked in this region. The measurements of the weight flow taken at three different points in the system are shown to be in good agreement.

Weight-flow data for tailpipes with the throat removed (fig. 7) and some data from figure 13 are compared with liquid flowmeter measurements in figure 14. From these data, discharge coefficients C_d (defined as the ratio of measured to theoretical weight flow calculated from the exhaust-gas measurements) have been determined. The average value of the discharge coefficient for these convergent nozzles is about 0.97, which is consistent with usual convergent-nozzle values (for example, ref. 19). This correspondence is an indication of uniform flow across the exit nozzle.

The relationship between propellant weight flow and jet pressure ratio for various sizes of convergent nozzles with a hydrogen peroxide jet-simulator system is shown in figure 15. The solid lines represent the ideal relationship for the decomposition products of 90 percent hydrogen peroxide calculated for the adiabatic decomposition temperature of 1,364° F and standard atmospheric conditions. The linear variation of jet pressure ratio with weight flow of propellant is illustrated for sonic nozzle conditions. In the actual case, the nozzle would not be choked below the critical pressure ratio of 1.32, and all the curves would fair into a jet-off pressure ratio of 1.0 since the flow is zero at this point. The test points shown (d_j = 2.62 in.) are measurements of the liquid hydrogen peroxide flow rate obtained from the electronic flowmeter. Calculated weight flows determined from measured exhaust gas pressures and temperatures are compared with the flowmeter measurements. The deviation of this calculated flow from the ideal values is attributable to use of the measured jet temperature which was lower than the adiabatic decomposition temperature and to a higher ambient pressure than standard.

The decomposition chamber was designed for a weight flow of 4 pounds per second, and the unit could pass weight flows up to 7 pounds per second with smooth and steady operation, with instant starts and stops being made once the propellant lines were filled. It has been found that for the decomposition-chamber size and flow rates used (average flow rate 2.5 lb/sec), the catalyst bed would last for about 1 hour before the bed deteriorated. With the exit nozzle shown in figure 7 (d_j = 2.62 in.) ratios of jet total pressure to ambient static pressure up to 5 could be easily established in the static test facility. It should be noted that pressure ratios considerably greater than those corresponding to turbojet operation at transonic speeds (ref. 20) can be obtained in atmospheric wind tunnels because of the decrease in static pressure with Mach number. This is illustrated in figure 16 where jet pressure ratios have been calculated for Mach numbers from 0 to 1.4 as a function of the ideal weight flow parameter w_i/A. The actual jet pressure ratios obtained in a simulator installation will depend upon the pressure losses in the induction system and the pressure available with the supply apparatus.

Thrust Measurements

The variation of jet thrust with pressure ratio is presented in figure 17 for a convergent nozzle having an exit diameter of 3.20 inches. Measured thrust is compared with the ideal convergent nozzle thrust and the ideal thrust for complete isentropic expansion of the primary flow. The ideal thrusts have been calculated from measured weight flows, jet total temperatures, and jet total pressures. The ratio of measured jet thrust to the ideal isentropic thrust is also shown in this figure and has an average value of about 0.97 for this nozzle.

The variation of static thrust coefficient $C_{F,o}$ with jet pressure ratio is presented in figure 18 for three convergent nozzles. The static thrust coefficient nondimensionalizes the data so that all sizes of nozzles should be on a single line. The differences between the nozzles are mainly due to differences in the nozzle discharge coefficients. The data presented in figures 17 and 18 indicate that the thrust values obtained with the jet simulator are in good agreement with the theoretical values for full-scale convergent nozzles.

CONCLUDING REMARKS

A hydrogen peroxide turbojet-engine-exhaust simulator for powered model testing in wind tunnels with air exchange has been developed. The hydrogen peroxide system provides a hot jet with characteristics that correspond closely to the exhaust of a turbojet engine. This system has the advantage of compactness, small propellant lines, and simple

control of the jet pressure ratio by varying the propellant flow rate. The necessary associated equipment needed to operate the system has been described. Static-test data obtained with the hydrogen peroxide system show that experimental results with convergent nozzles are in good agreement with theoretical values and are consistent with convergent nozzle discharge and thrust coefficients.

Langley Research Center,
National Aeronautics and Space Administration,
Langley Field, Va., September 18, 1958.

REFERENCES

1. Salmi, Reino J.: Experimental Investigation of Drag of Afterbodies With Exiting Jet at High Subsonic Mach Numbers. NACA RM E54I13, 1954.

2. Rousso, Morris D., and Baughman, L. Eugene: Spreading Characteristics of a Jet Expanding From Choked Nozzles at Mach 1.91. NACA TN 3836, 1956.

3. Englert, Gerald W., and Luidens, Roger W.: Wind-Tunnel Technique for Simultaneous Simulation of External Flow Field About Nacelle Inlet and Exit Airstreams at Supersonic Speeds. NACA TN 3881, 1957.

4. De Moraes, Carlos A., Hagginbothom, William K., Jr., and Falanga, Ralph A.: Design and Evaluation of a Turbojet Exhaust Simulator, Utilizing a Solid-Propellant Rocket Motor, for Use in Free-Flight Aerodynamic Research Models. NACA RM L54I15, 1954.

5. Cahn, Maurice S.: An Experimental Investigation of Sting-Support Effects on Drag and a Comparison With Jet Effects at Transonic Speeds. NACA Rep. 1353, 1958. (Supersedes NACA RM L56F18a, 1956.)

6. Lee, George, and Summers, James L.: Effects of Sting-Support Interference on the Drag of an Ogive-Cylinder Body With and Without a Boattail at 0.6 to 1.4 Mach Number. NACA RM A57I09, 1957.

7. Evans, Albert J.: The Simulation of the Effects of Internal Flow in Wind Tunnel Model Tests of Turbojet Powered Aircraft. Papers Presented at Seventh Meeting of the Wind Tunnel and Model Testing Panel, Ottawa, Canada. AG19/P9, AGARD, North Atlantic Treaty Organization, June 1955, pp. 53-68.

8. Sutton, George P.: Rocket Propulsion Elements. Second ed., John Wiley & Sons, Inc., c.1956.

9. Bloom, Ralph, Jr., Davis, Noah S., Jr., and Levine, Samuel D.: Hydrogen Peroxide as a Propellant. Jour. Am. Rocket Soc., no. 80, Mar. 1950, pp. 3-17.

10. Li, T. Y., Yoler, Y. A., and Morgan, A. J. A.: The Design of Wind Tunnel Experiments for the Study of Jet-On Effects. NAVORD Rep. 3473 (NOTS 1081), U. S. Naval Ord. Test Station (China Lake, Calif.), Apr. 12, 1955.

11. Love, Eugene S., and Grigsby, Carl E.: Some Studies of Axisymmetric Free Jets Exhausting From Sonic and Supersonic Nozzles Into Still Air and Into Supersonic Streams. NACA RM L54L31, 1955.

12. Bressette, Walter E., and Faget, Maxime A.: An Investigation of Jet Effects on Adjacent Surfaces. NACA RM L55E06, 1955.

13. Anon.: Hydrogen Peroxide Physical Properties Data Book. Second ed. Bull. No. 67, Food Machinery and Chemical Corp., BECCO Chemical Div. (Buffalo), 1955.

14. Wentworth, R. L.: The Mechanism of the Catalytic Decomposition of Hydrogen Peroxide by Silver. Rep. No. 32, D.I.C. 6552 (Contract No. N5ori-07819), M.I.T., May 1, 1951.

15. Kochendorfer, Fred D.: Effect of Properties of Primary Fluid on Performance of Cylindrical Shroud Ejectors. NACA RM E53L24a, 1954.

16. Anon.: Handbook - Field Handling of Concentrated Hydrogen Peroxide (Over 52 Weight Percent Hydrogen Peroxide). NAVAER 06-25-501, Bur. Aero., July 1, 1955. (Rev. Jan. 15, 1957.)

17. Davis, Noah S., Jr., and Keefe, John H., Jr.: Equipment for Use With High-Strength Hydrogen Peroxide. Jour. Am. Rocket Soc., vol. 22, no. 2, Mar.-Apr. 1952, pp. 63-69.

18. Sanders, John C., Novik, David, and Hart, Clint E.: Effect of Dynamic Characteristics of Rocket Components on Rocket Control. Aero. Eng. Rev., vol. 16, no. 10, Oct. 1957, pp. 73-77.

19. Huntley, S. C., and Yanowitz, Herbert: Pumping and Thrust Characteristics of Several Divergent Cooling-Air Ejectors and Comparison of Performance With Conical and Cylindrical Ejectors. NACA RM E53J13, 1954.

20. Cortright, Edgar M., Jr.: Some Aerodynamic Considerations of Nozzle-Afterbody Combinations. Aero. Eng. Rev., vol. 15, no. 9, Sept. 1956, pp. 59-65.

TABLE I

COMPARISONS OF JET EXHAUST PARAMETERS

Type jet	Altitude, ft	p_∞, lb/sq ft	q_∞, lb/sq ft	T_∞, $^\circ R$	$\frac{p_j}{p_\infty}$	$\frac{w_i/A, \text{lb/sec}}{\text{sq ft}}$	$\frac{F_{i,c}}{A}$, lb/sq ft	C_F	$T_{t,j}$, $^\circ R$	γ	R, ft/$^\circ R$	V_j, ft/sec	$\frac{V_j}{V_\infty}$	δ, deg	$\frac{r}{d_j}$
Take-off static thrust (nonafterburning); $M_\infty = 0$; $\frac{p_{t,j}}{p_\infty} = 2.60$															
Turbojet	0	2,121	---	520	1.40	68.0	4,148	----	1,600	1.345	53.40	1,775	----	6.6	[a]10.8
Air	0	2,121	---	520	1.37	134.6	5,054	----	520	1.40	53.30	1,020	----	5.5	[a]13.6
H_2O_2	0	2,121	---	520	1.43	58.0	4,750	----	1,824	1.27	69.89	2,140	----	6.4	[a]8.1
Cruising flight (nonafterburning); $M_\infty = 0.85$; $\frac{p_{t,j}}{p_\infty} = 4.20$															
Turbojet	35,000	498	252	394	2.25	28.3	2,003	7.95	1,325	1.36	53.28	1,620	1.96	15.5	3.70
[b]Air	12,400	1,322	669	560	2.22	129.5	5,715	8.54	520	1.40	53.30	1,020	1.15	14.0	3.70
[b]H_2O_2	12,400	1,322	669	560	2.32	56.0	5,600	8.37	1,824	1.27	69.89	2,140	2.41	17.1	3.67
Afterburning climb; $M_\infty = 1.10$; $\frac{p_{t,j}}{p_\infty} = 5.20$															
Turbojet	45,000	309	261	392	2.84	16.5	2,050	7.85	3,250	1.30	53.50	2,515	2.35	20.8	3.3
[b]Air	19,500	993	841	610	2.75	120.5	5,557	6.61	520	1.40	53.30	1,020	.92	19.0	3.3
[b]H_2O_2	19,500	993	841	610	2.87	54.0	5,447	6.48	1,824	1.27	69.89	2,140	1.94	21.6	3.3

[a]Estimation of r/d_j difficult and relatively unimportant in this case inasmuch as the curves become asymptotic at low values of pressure ratio. (See fig. 2.)

[b]Equivalent values for atmospheric wind tunnel.

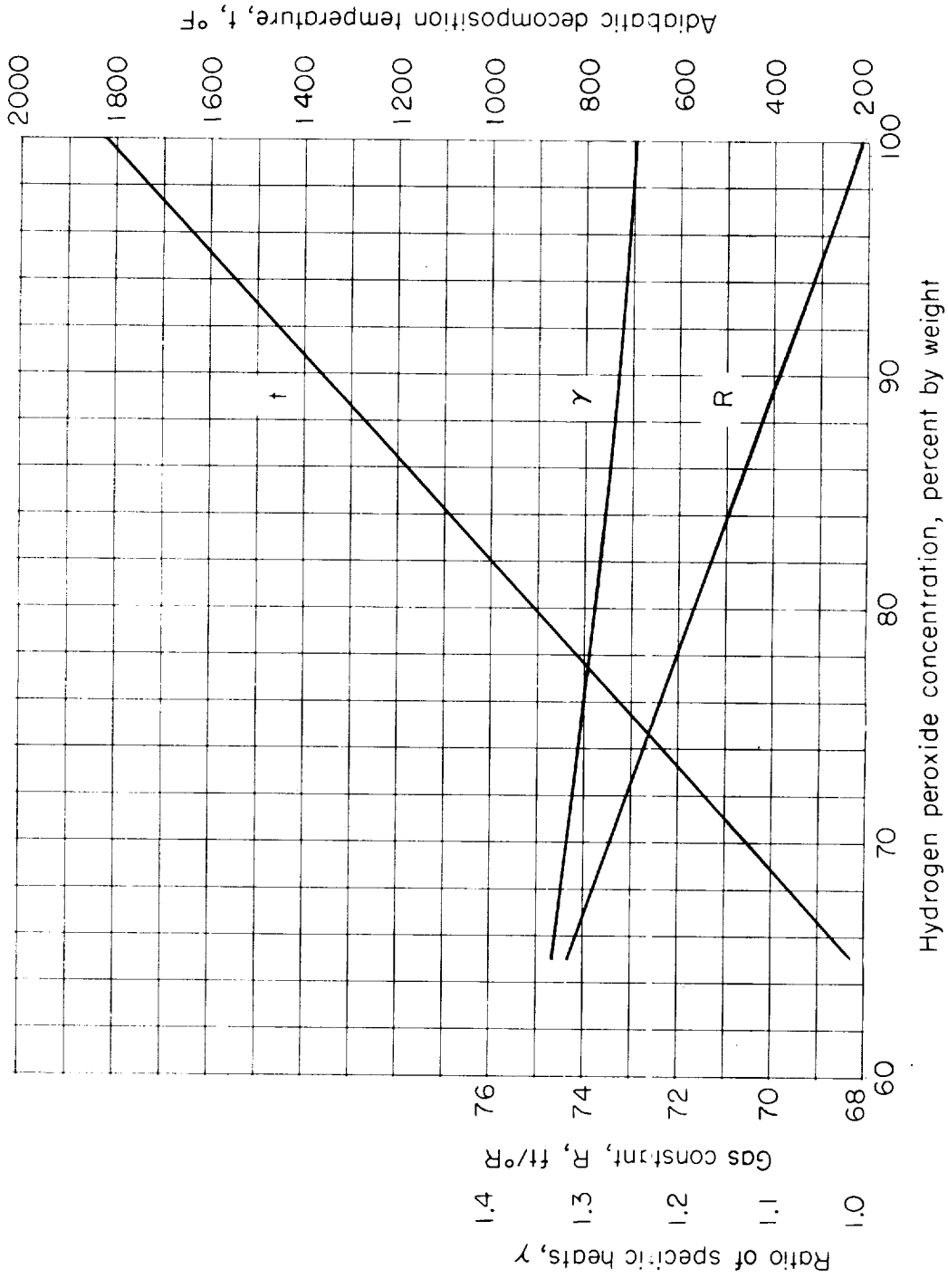

Figure 1.- Physical properties of hydrogen peroxide decomposition products. Adiabatic decomposition of unconfined system at 1.0 atmosphere.

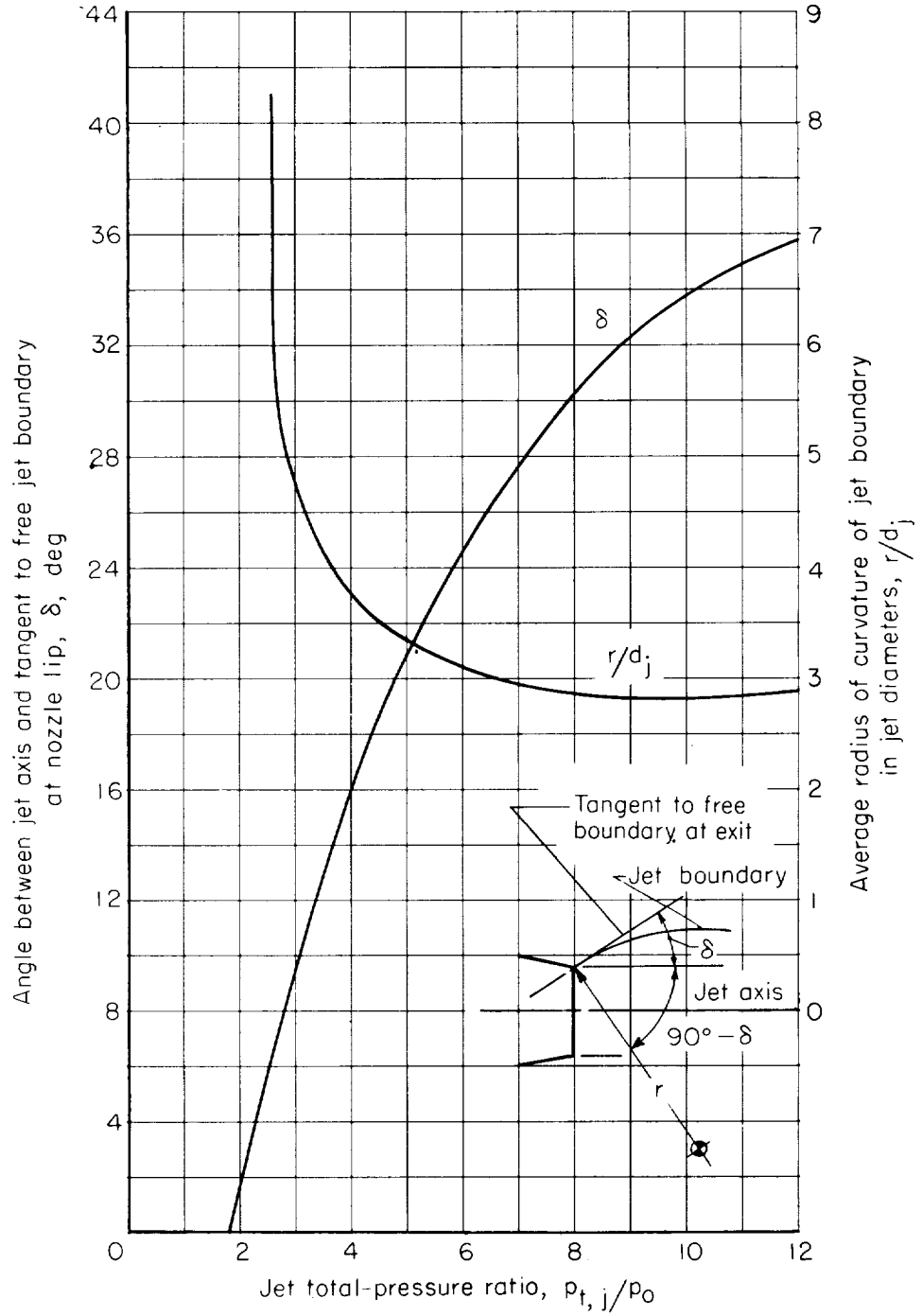

Figure 2.- Jet-boundary shape parameters for 90 percent by weight hydrogen peroxide decomposition products. Convergent nozzle exhausting into still air. $M_j = 1.0$; $\gamma = 1.27$.

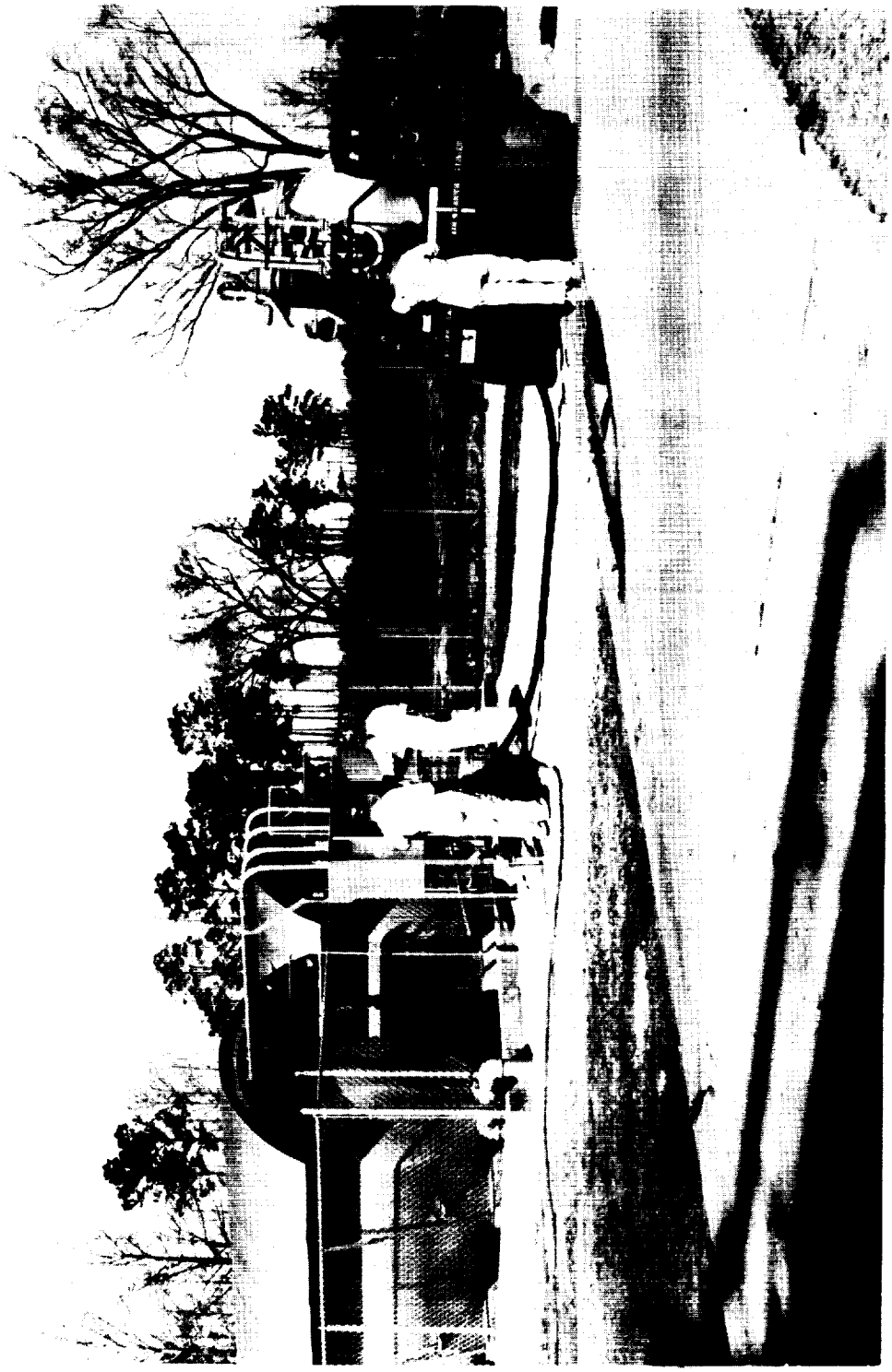

Figure 3.- Hydrogen peroxide storage tanks and portable supply system. L-88693

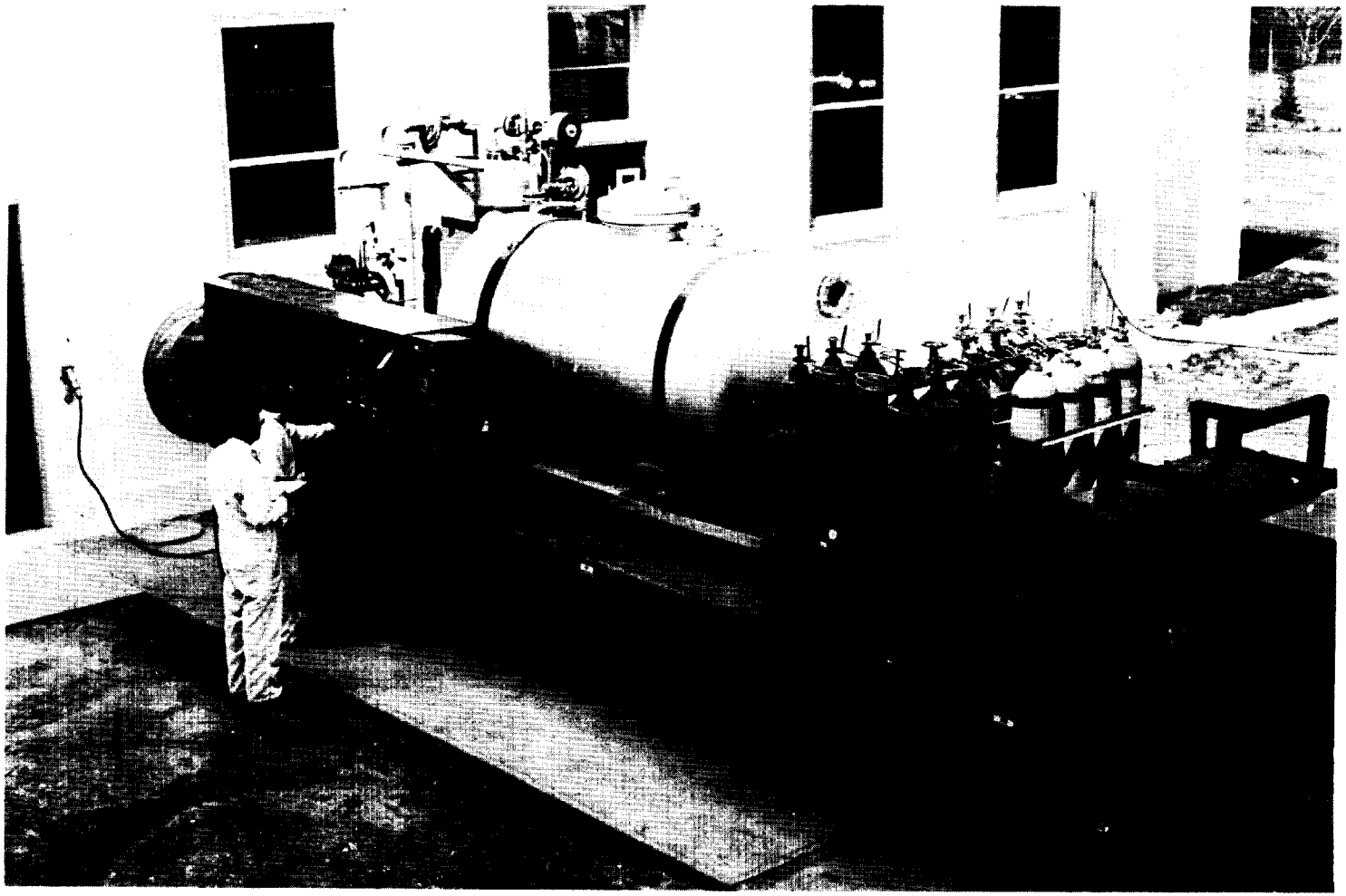

Figure 4.- Trailer-mounted hydrogen peroxide supply system. L-88783

OPERATION

1. Pump H_2O_2 from storage tank to vented high-pressure tank
2. Close vent; pressurize 30-gallon tank with nitrogen
3. Open run valve and set throttle valve for proper flow rate for desired pressure ratio
4. When flow has stabilized at required pressure ratio (5 sec), take data record (5 sec)
5. Repeat step 4 for other pressure ratios
6. Close run valve

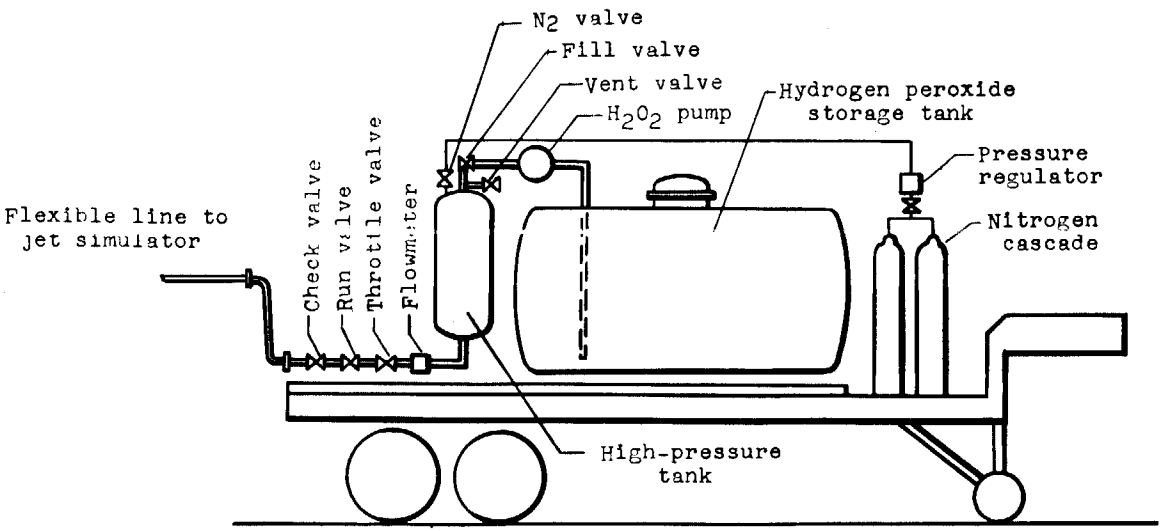

Figure 5.- Schematic sketch of portable hydrogen peroxide supply system and operating sequence.

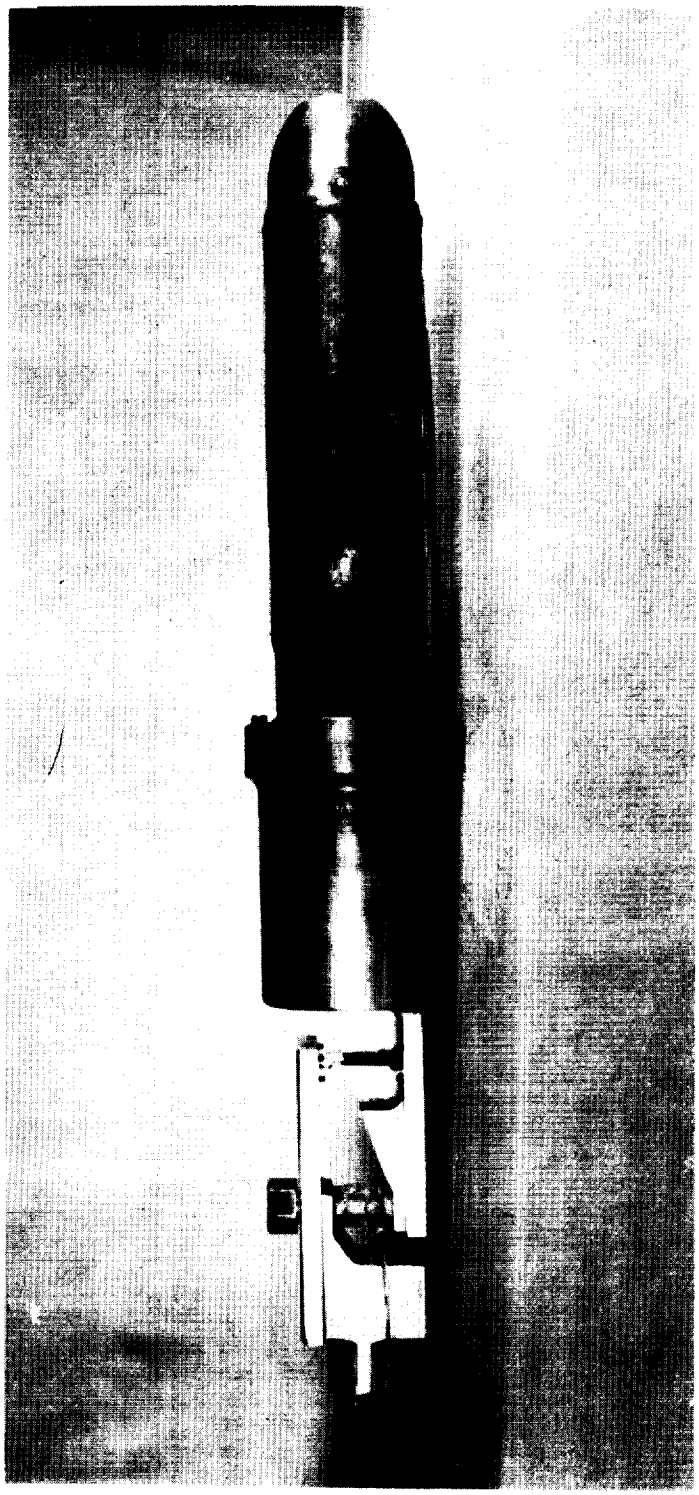

Figure 6.- Photograph of a hydrogen peroxide jet simulator. L-58-1953.1

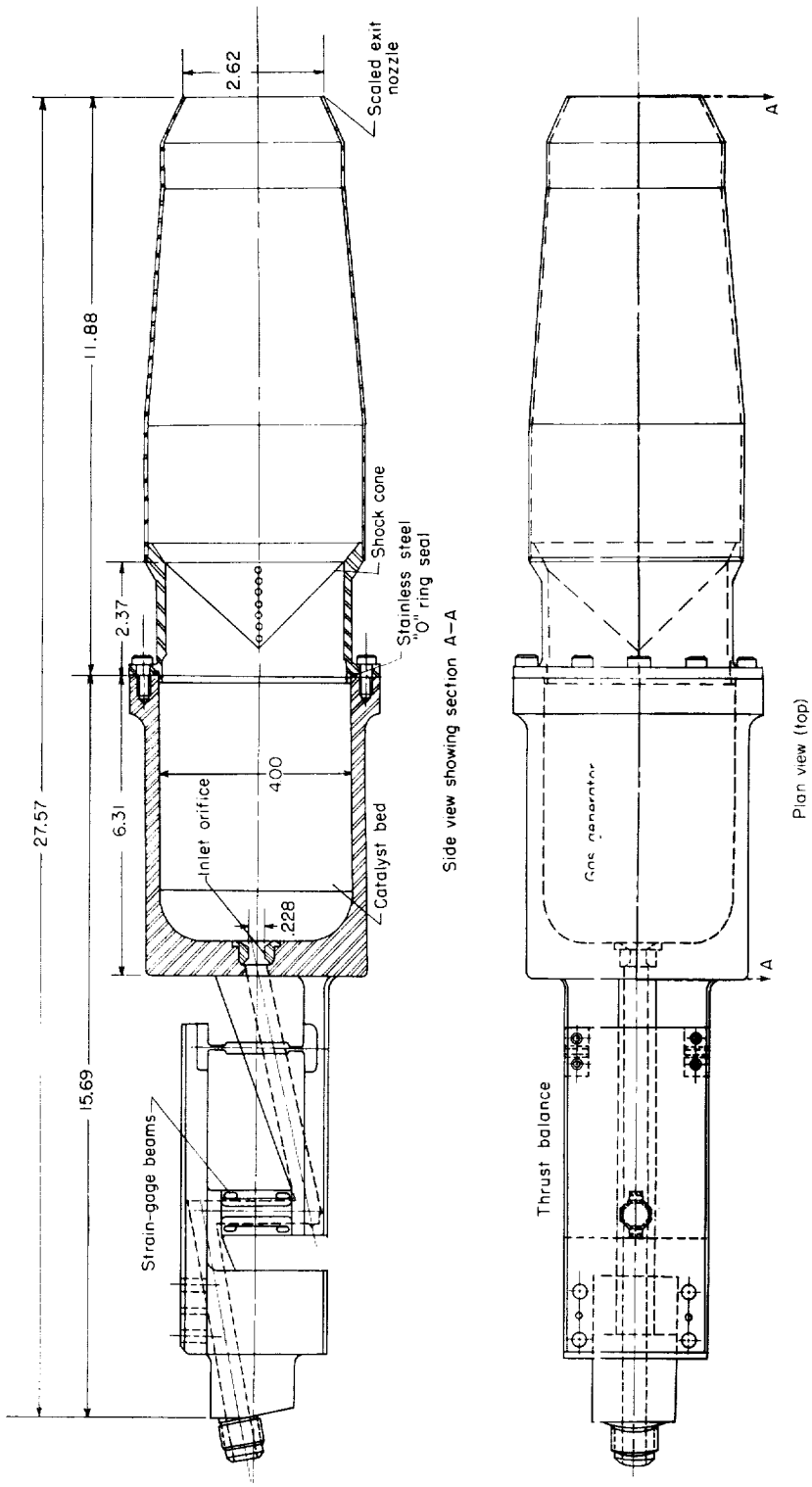

Figure 7.- Details of hydrogen peroxide gas generator and thrust balance system. (All dimensions are in inches.)

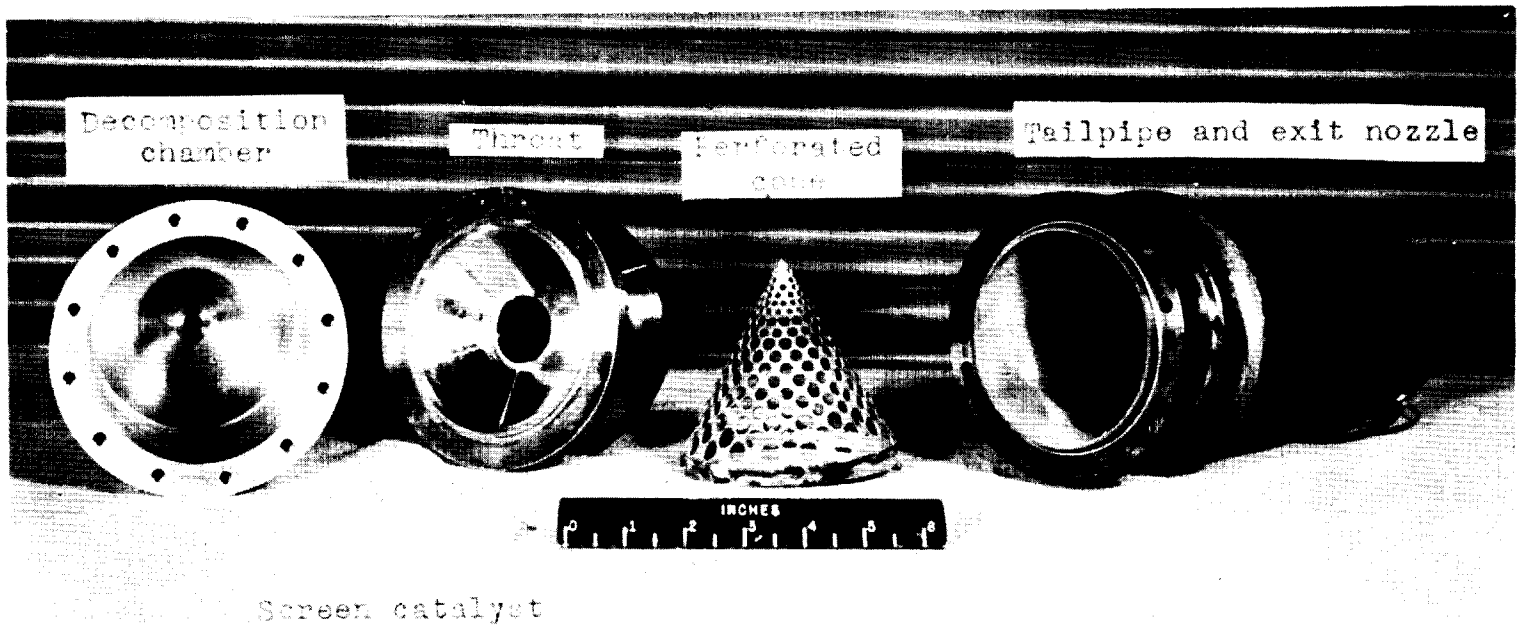

L-96668.1

Figure 8.- Photograph of components of the gas-generator—tailpipe system.

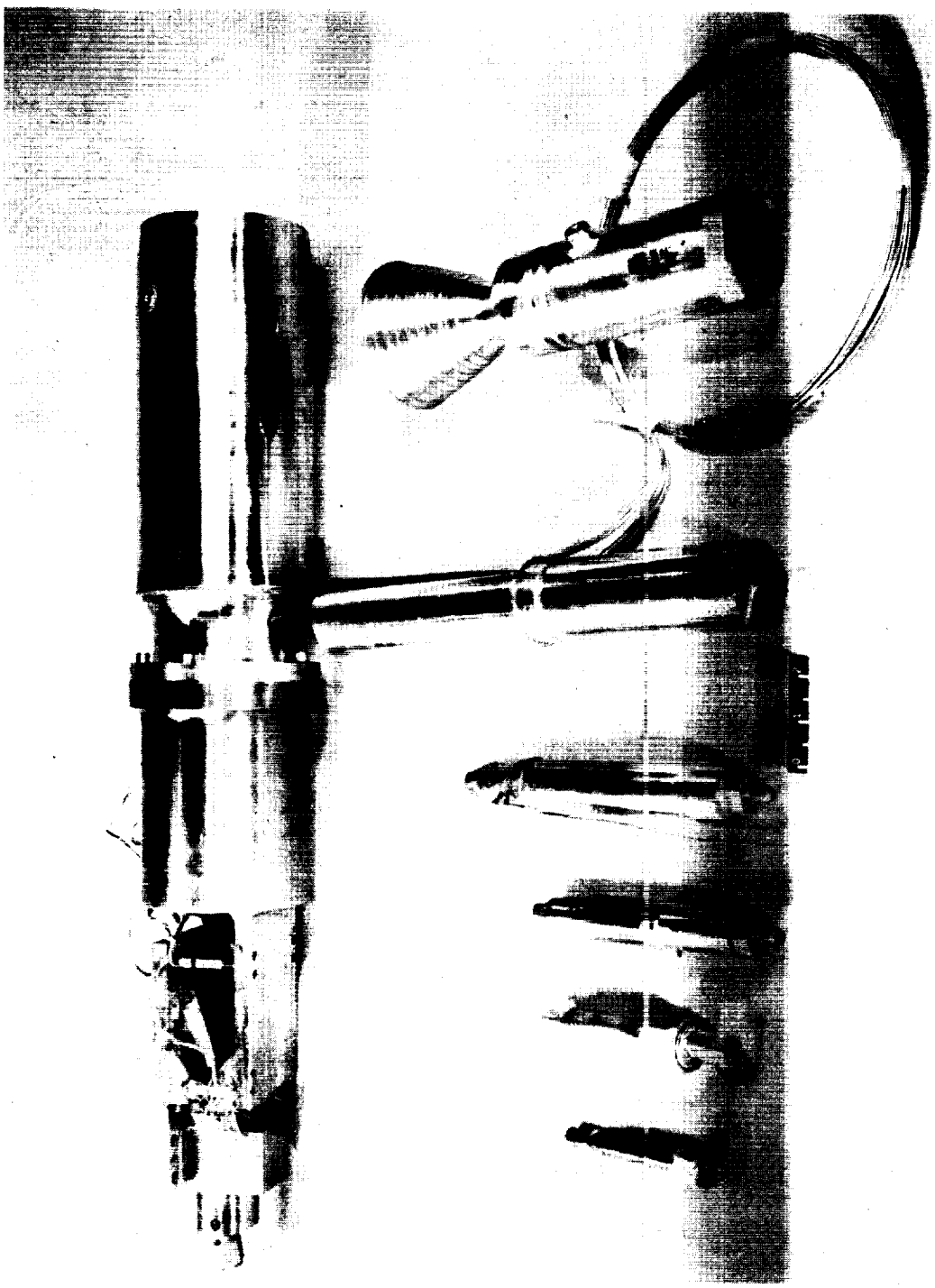

Figure 9.- Hydrogen peroxide gas-generator units. L-57-2561

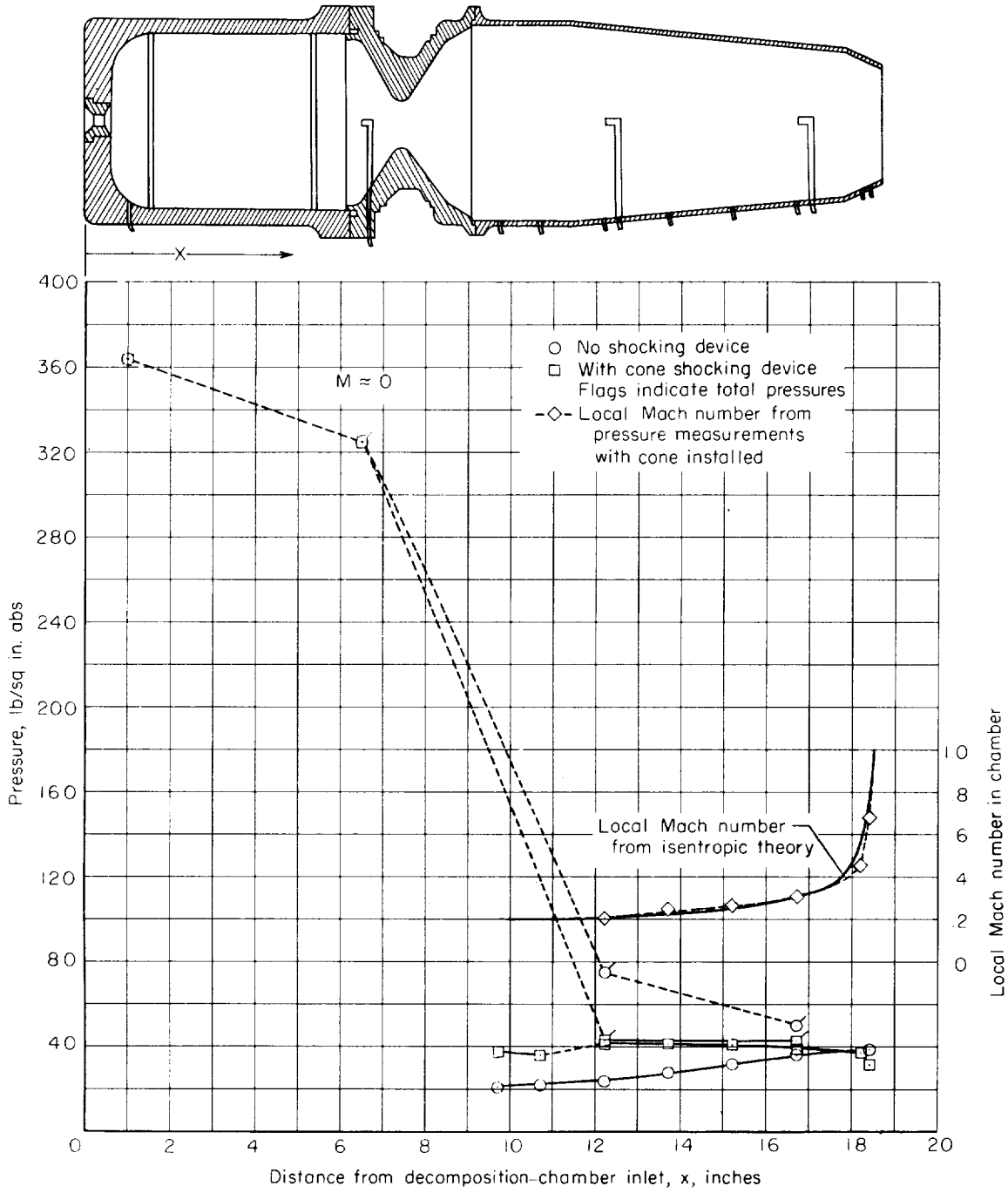

Figure 10.- Variation of measured internal pressure along jet simulator.

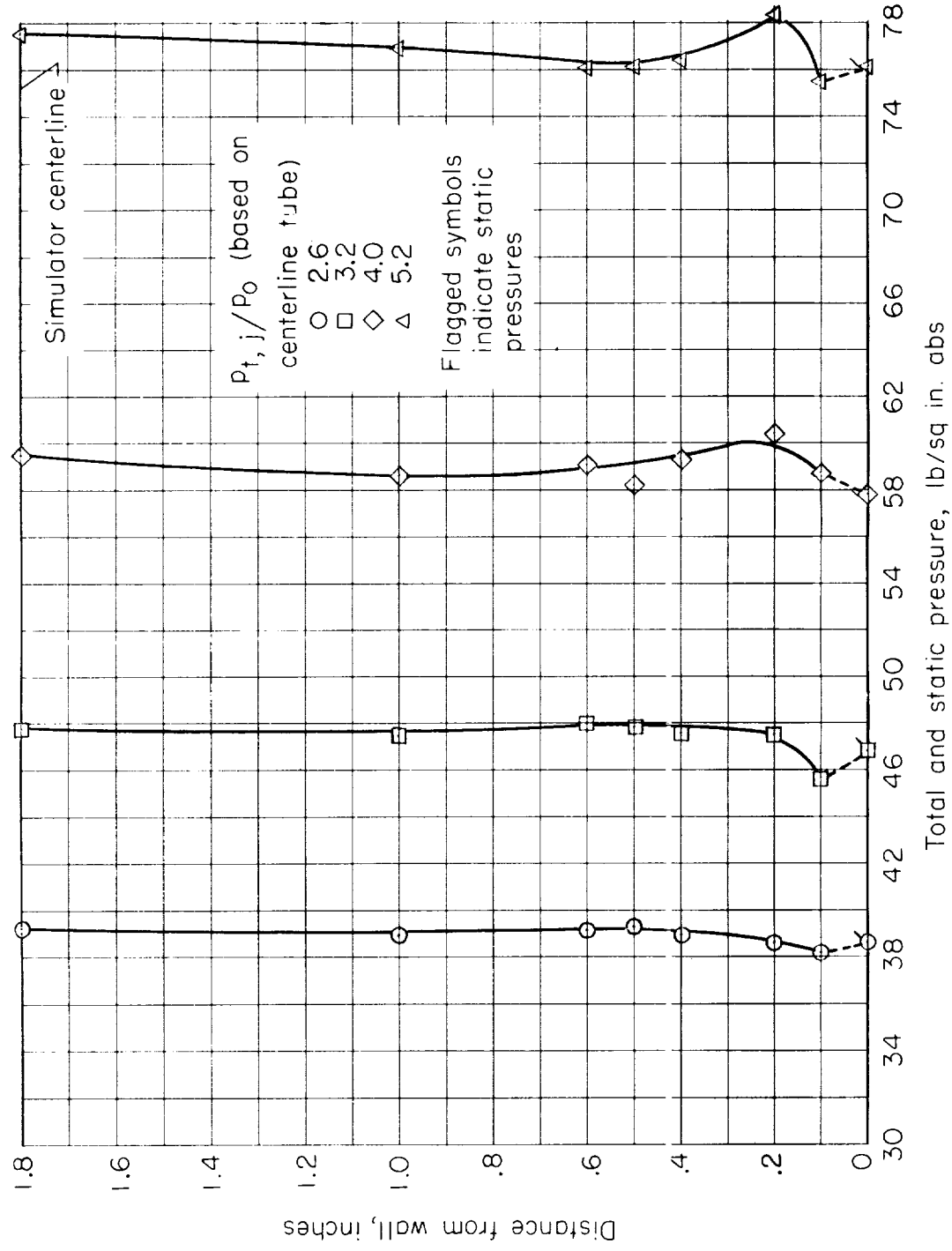

Figure 11.- Total-pressure variation at x = 16.7 inches from simulator wall to center line at several jet total-pressure ratios. Flagged symbols are wall static pressures.

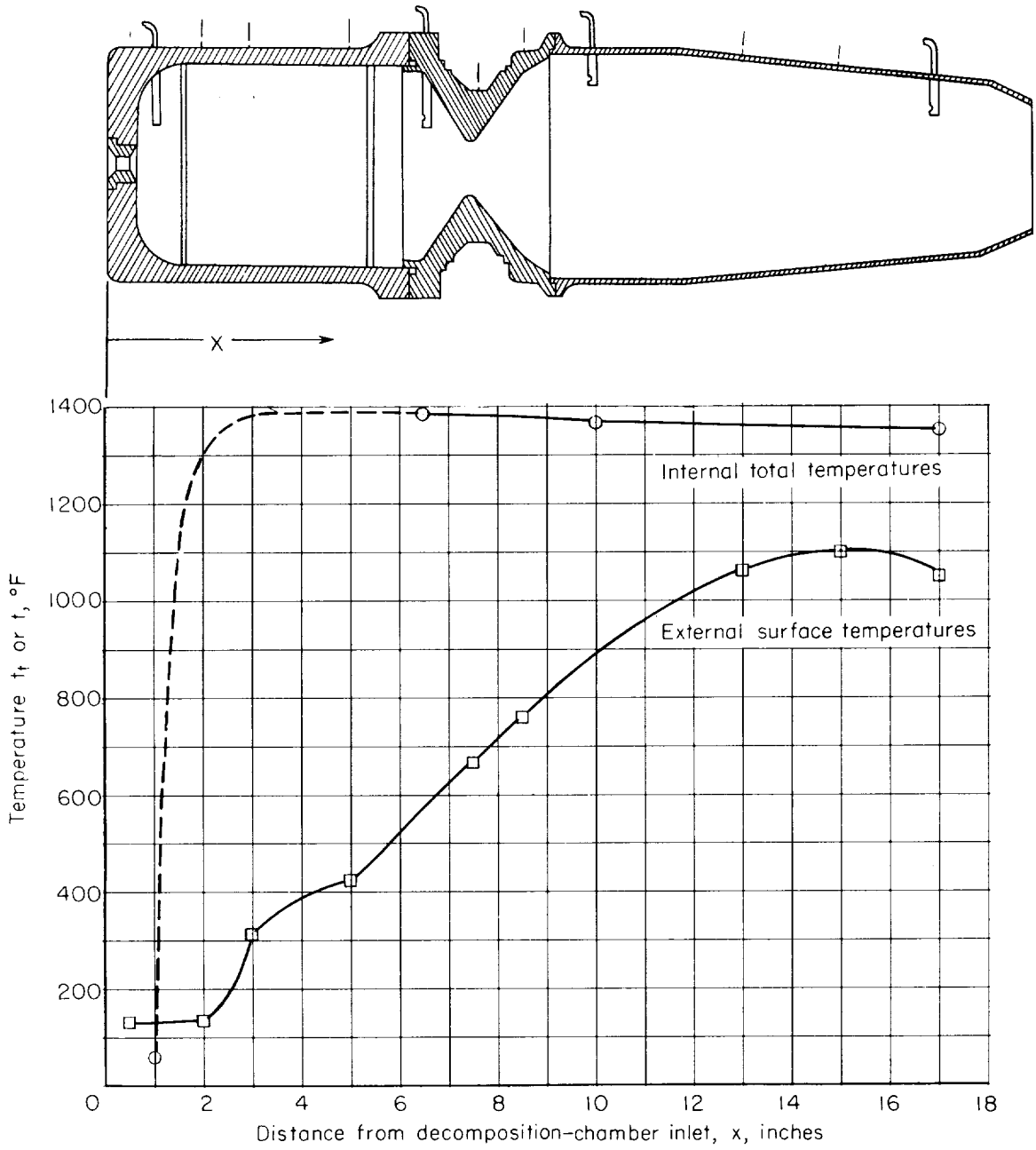

Figure 12.- Typical variation of temperature along jet simulator system. Primary system only. $t_o = 62^\circ$ F; $p_{t,j}/p_o = 2.8$.

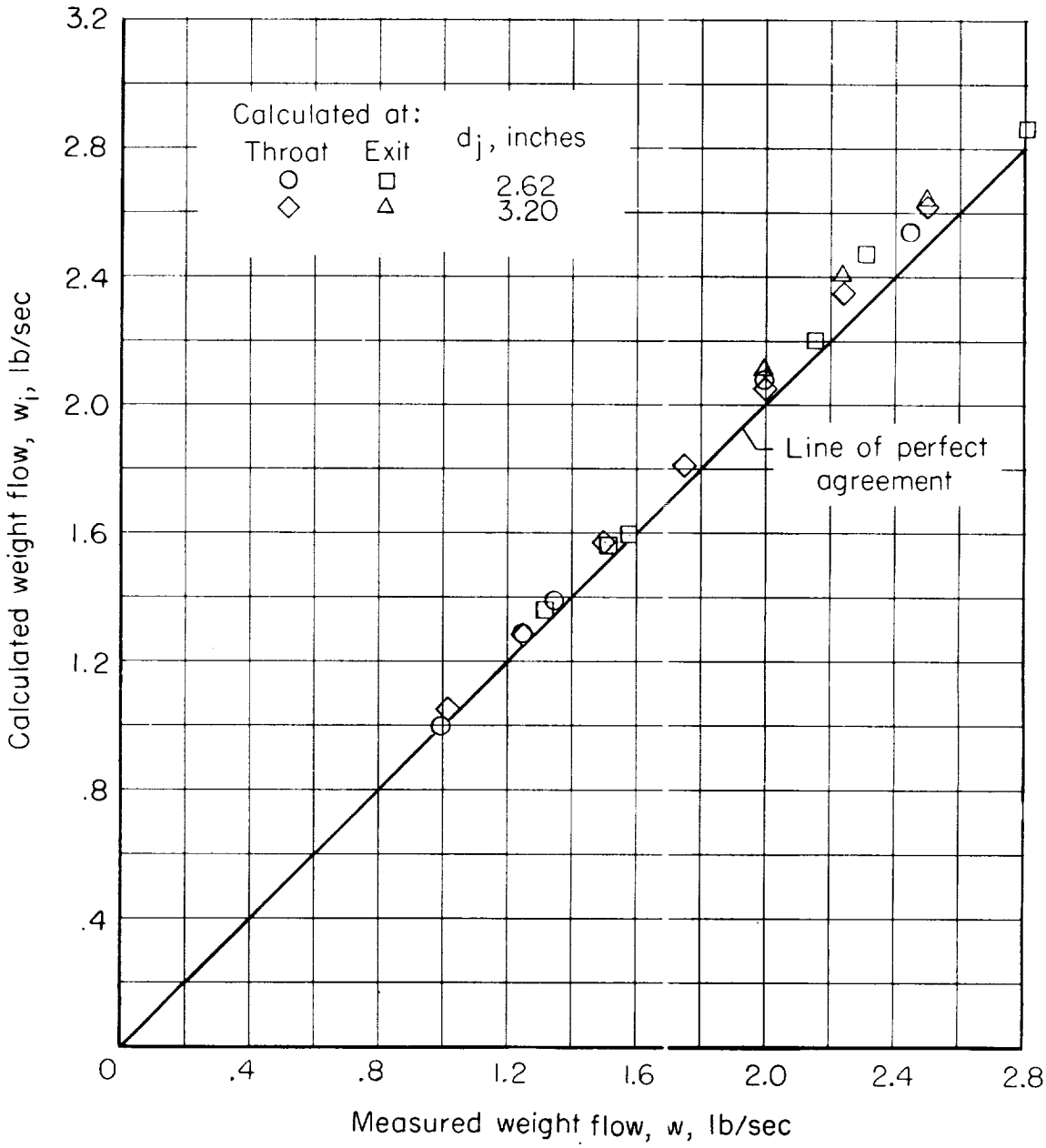

Figure 13.- Comparison of flow rates calculated from gas measurements with liquid-flowmeter measurements. Convergent nozzles.

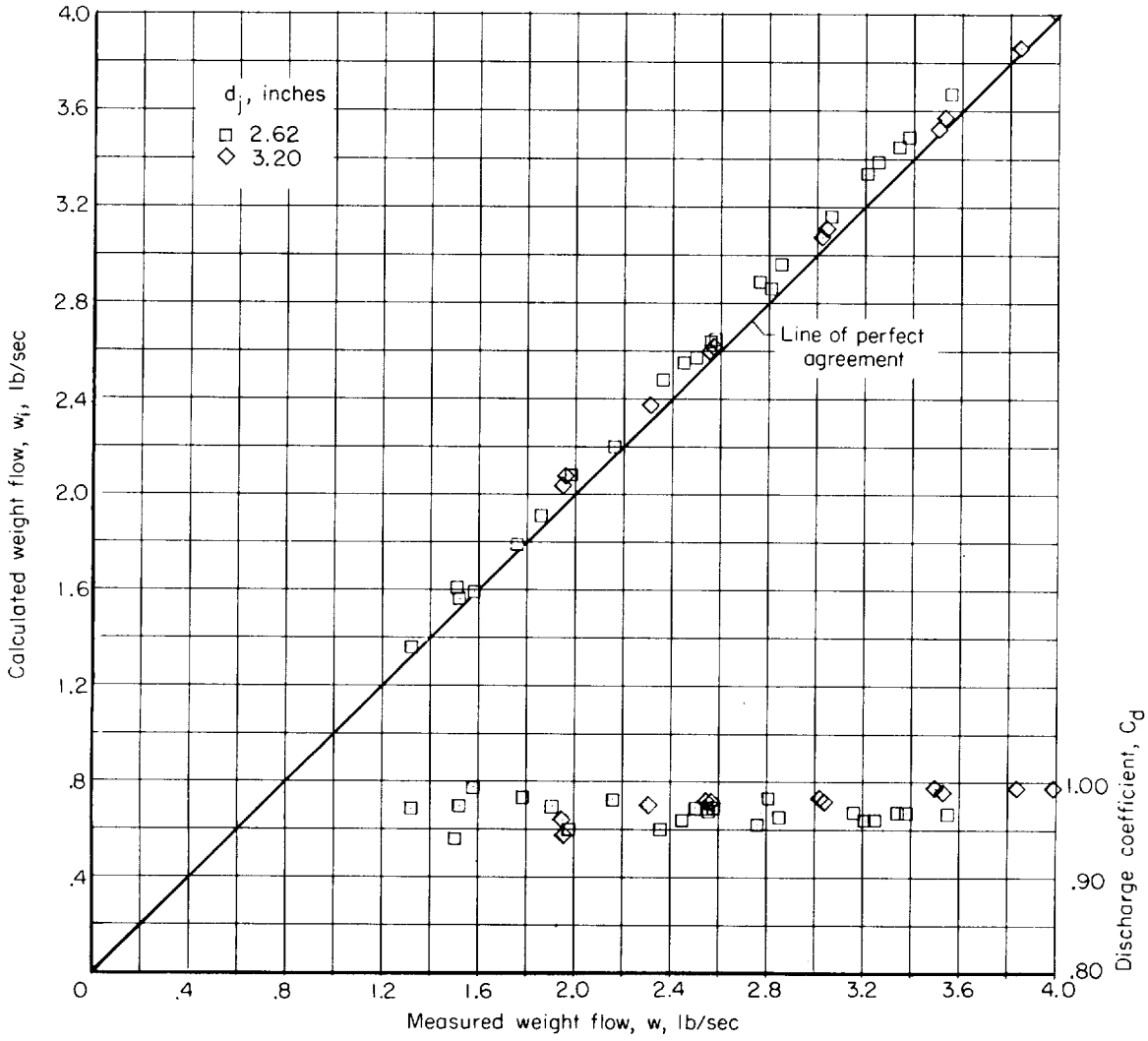

Figure 14.- Discharge coefficient for sonic nozzles.

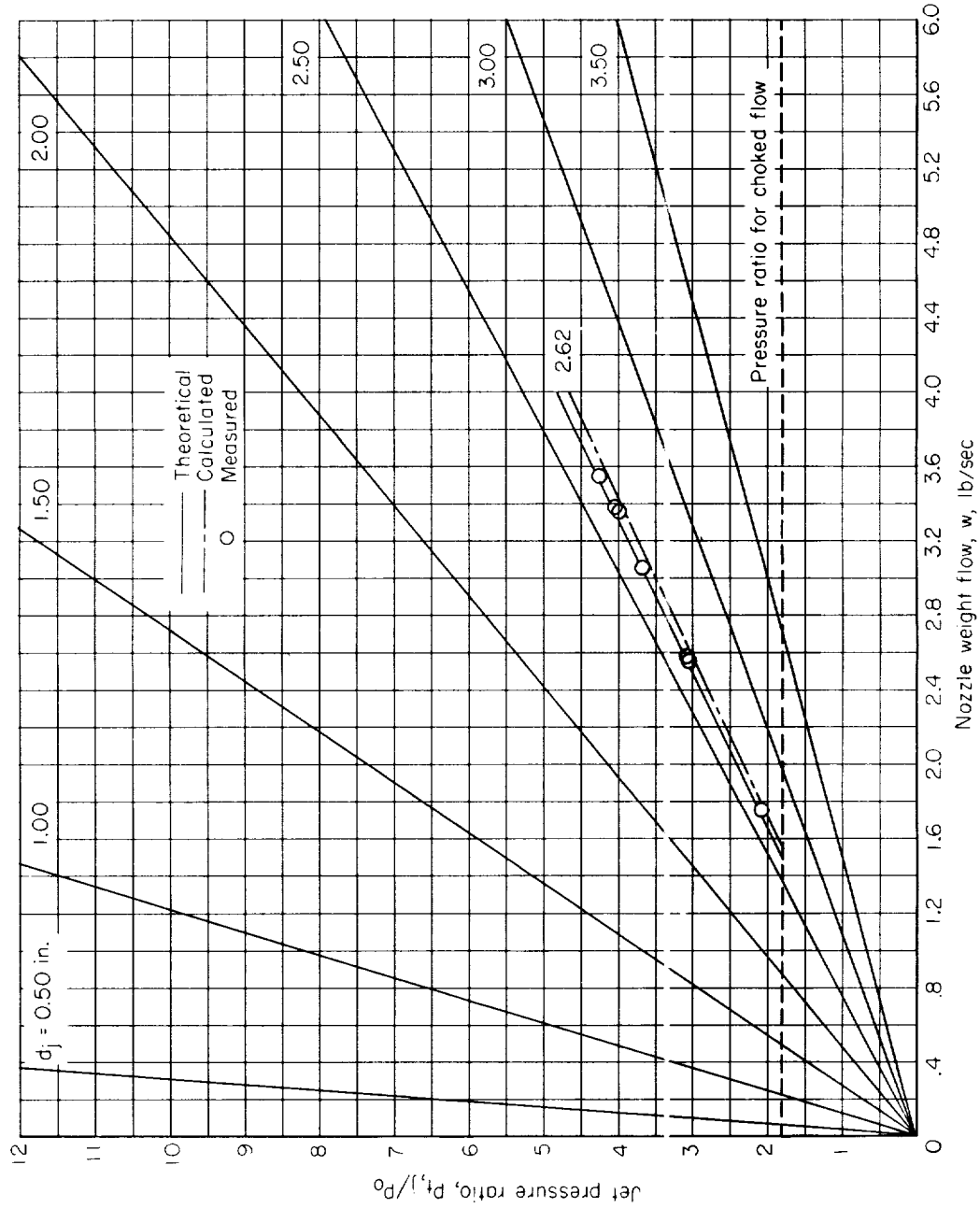

Figure 15.- Variation of jet pressure ratio with nozzle weight flow for convergent sonic nozzles with 90 percent concentration hydrogen peroxide jets. Standard sea-level conditions.

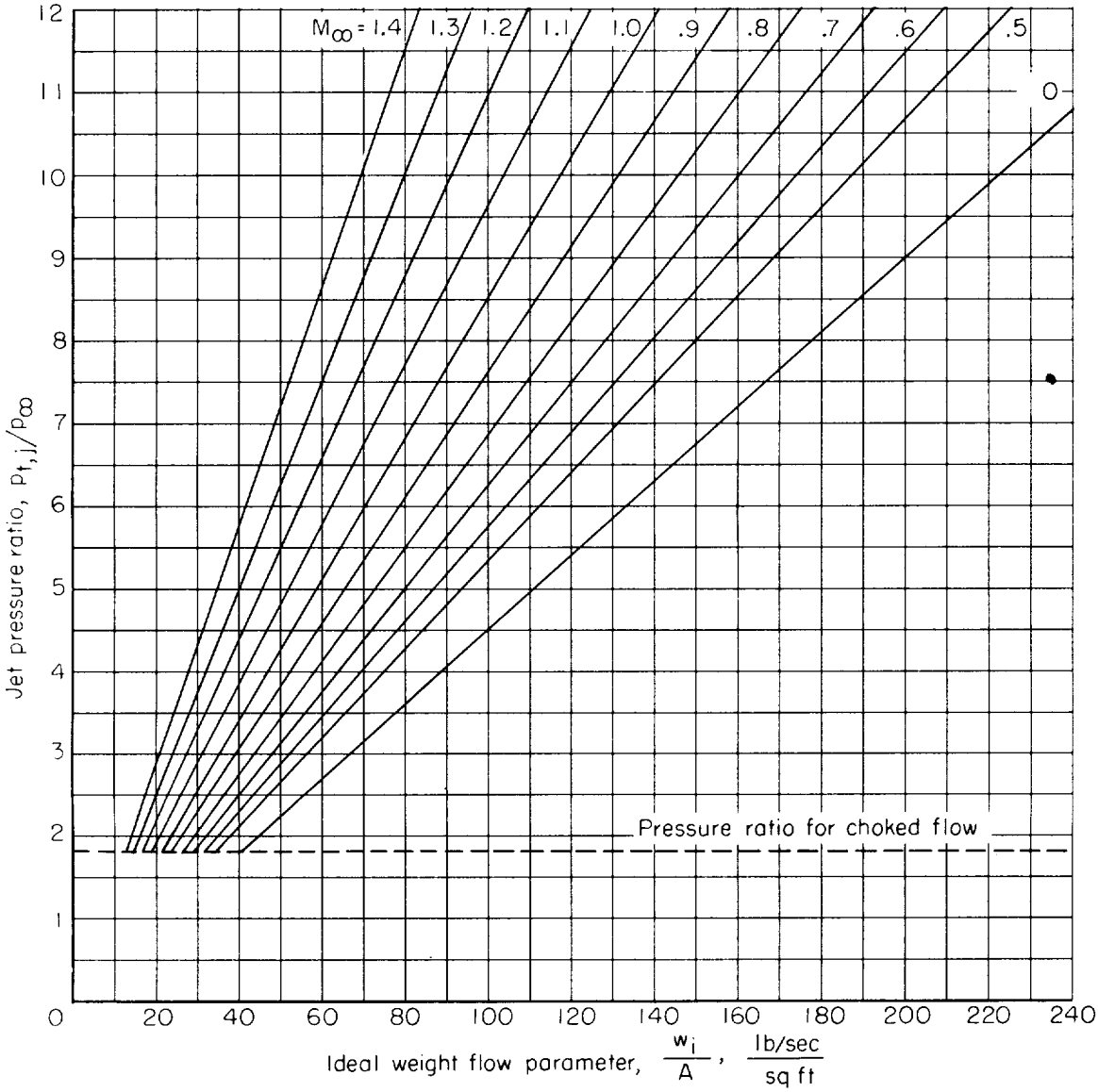

Figure 16.- Weight flows required to obtain jet pressure ratios at various Mach numbers in atmospheric wind tunnels.

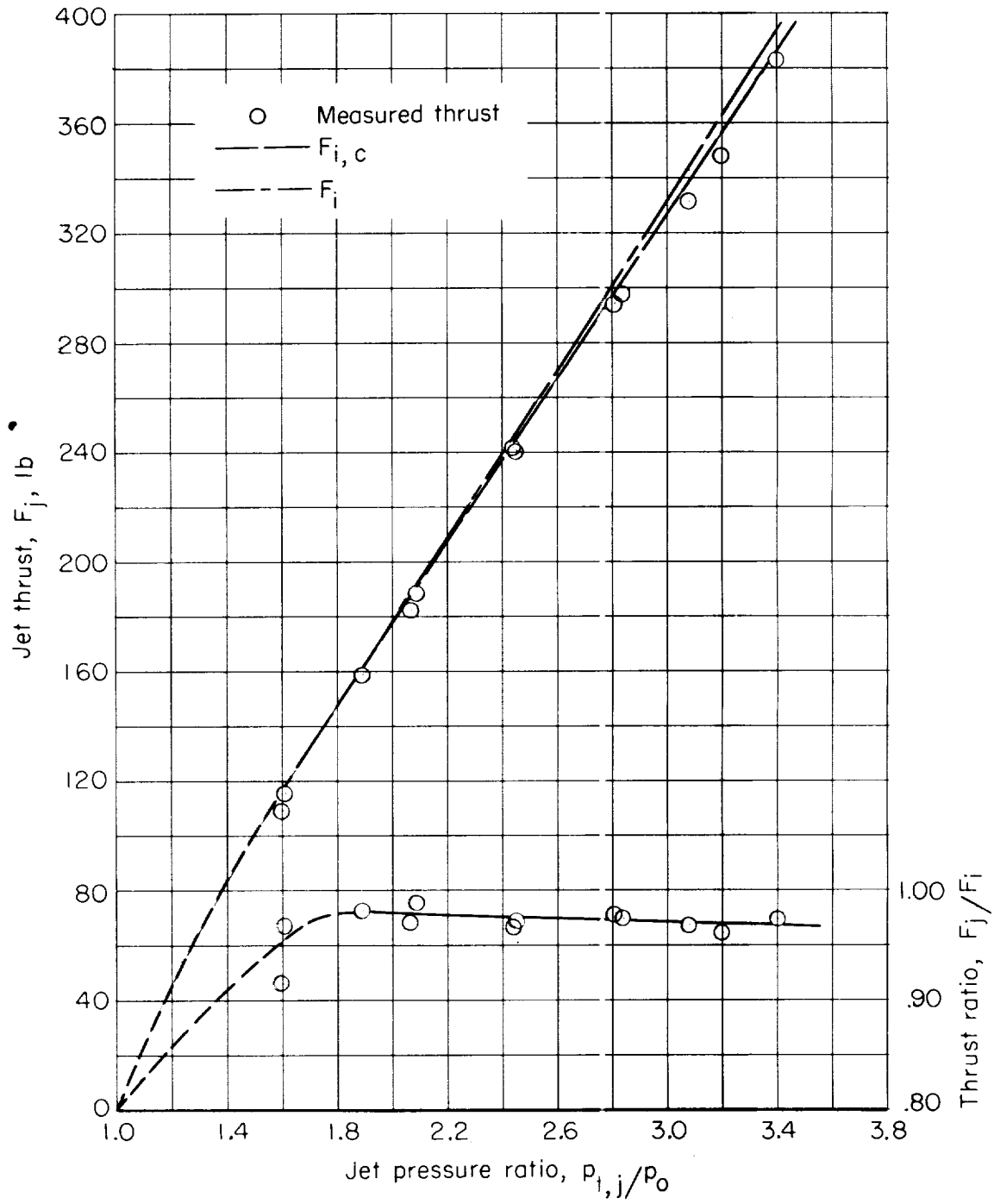

Figure 17.- Variation of jet thrust and thrust ratio with pressure ratio. Convergent nozzle; d_j = 3.20 inches.

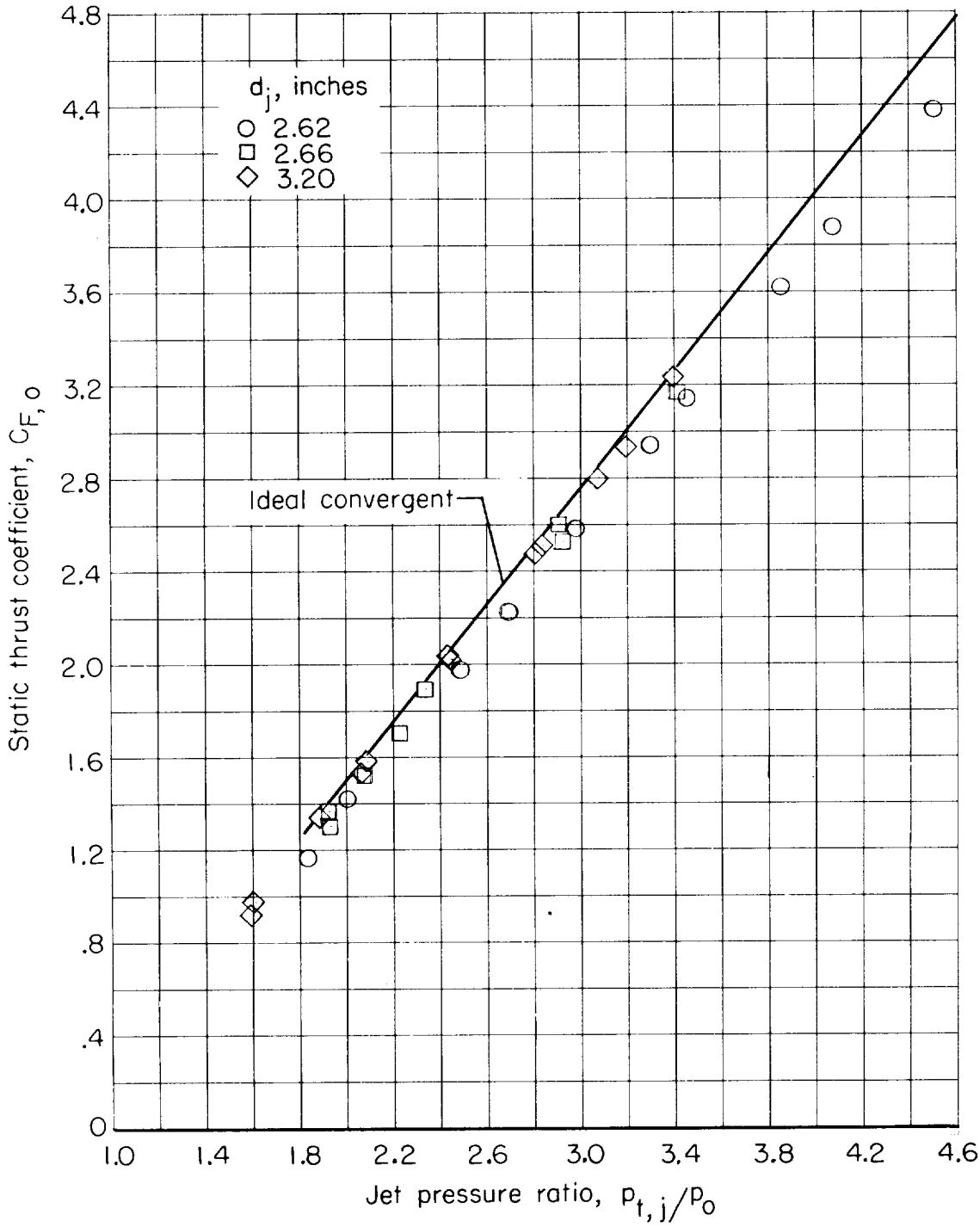

Figure 18.- Variation of static thrust coefficient with jet pressure ratio for several convergent nozzles.

NASA - Langley Field, Va. L-110